

First-Principles Simulations of Violent Space-Weather Events

C.R. DeVore¹ and S.K. Antiochos²

¹Laboratory for Computational Physics and Fluid Dynamics

²Space Weather Laboratory, NASA Goddard Space Flight Center

We have developed a first-principles model for simulating the initiation and propagation of magnetic eruptions originating in the Sun's atmosphere. The ejecta from these violent events adversely affect military and civilian facilities and operations on Earth. Energetic particles and radiation also pose prompt, direct hazards to technological systems and humans in space. Recently we have demonstrated that slow, coherent motions across the solar surface can energize susceptible magnetic field configurations and power subsequent catastrophic eruptions. The velocities and energies of our simulated events compare favorably with those observed, as do their morphological magnetic-field and plasma signatures. Our results also exhibit homology (repeated similar events originating from a single source), prompt reformation of the source region in the low solar atmosphere, and a magnetic-bottle configuration of the ejected field in the interplanetary medium. A fundamental understanding of these phenomena is a prerequisite for future physics-based forecasting of space weather.

INTRODUCTION

The U.S. Navy relies heavily, as does our society at large, on technological systems whose operations are susceptible to disturbances in the physical environment at Earth's surface, in the atmosphere, and in space. Certainly the most familiar of these, to both sailors and the general public, are unfavorable conditions in terrestrial weather: high or low temperatures, strong winds, heavy rain or snow, and high seas, for example. Less obvious but also important are the unavoidable and in some cases unpredictable changes in Earth's electromagnetic field and in the properties of the electrically charged gases (plasmas) that comprise its ionosphere and magnetosphere. These changes are driven, for the most part, by fluctuations in the flow of magnetic field and plasma from the Sun—the solar wind. The effects of these changes can include direct damage by energetic particles to orbiting satellites, astronauts, and pilots and crew in high-altitude aircraft; disruptions of ground-to-space-to-ground and ground-to-ground wireless communications; power blackouts due to voltage spikes in terrestrial power grids; and the occasionally spectacular, and always far more benign, auroral displays. The study of these changes, their origin at the Sun, and their consequences at Earth—both natural and technological—constitutes the emerging science of space weather.

The source of the most unpredictable and detrimental space weather is also the most violent: giant explosions of magnetic field and plasma from just above the visible surface of the Sun, which then propa-

gate out into interplanetary space at high speed and strike the Earth if it happens to lie in the path of the storm. One way to characterize the typical magnitude of these events is “a billion tons of matter moving at a million miles per hour,” or 1×10^{15} g at 500 km s^{-1} . The corresponding energy content is over 1×10^{30} ergs, equivalent to the yield of about a million 30-megaton nuclear weapons. Fortunately, that energy is spread over an enormous area by the time it reaches the Earth, so that only about one millionth of it actually enters the magnetosphere. This small fraction is, however, still more than sufficient to wreak significant havoc.

As is the case with devastating terrestrial-weather phenomena such as hurricanes, tornadoes, and blizzards, it would be highly advantageous to the military and to civilian society to be able to forecast the occurrence of these most damaging space-weather events. Satellites could be put into safe mode to protect their electronics; astronauts, pilots, and crew could be sheltered from adverse particle and radiation fluxes; alternative means of communications could be employed or operations could be accelerated or delayed; operators of power plants could adopt a defensive posture against electrical surges. At this time, however, we are limited to empirically based warnings of event onset at the Sun, and to several hours to perhaps two days notice of the arrival of the streaming ejecta at Earth. Both types of forecasts suffer from substantial uncertainties due to a relative paucity of data and an incomplete understanding of the physics of space weather. We are at a disadvantage relative to terrestrial-weather forecasters due to the impracticality of placing weather stations

Report Documentation Page				Form Approved OMB No. 0704-0188	
Public reporting burden for the collection of information is estimated to average 1 hour per response, including the time for reviewing instructions, searching existing data sources, gathering and maintaining the data needed, and completing and reviewing the collection of information. Send comments regarding this burden estimate or any other aspect of this collection of information, including suggestions for reducing this burden, to Washington Headquarters Services, Directorate for Information Operations and Reports, 1215 Jefferson Davis Highway, Suite 1204, Arlington VA 22202-4302. Respondents should be aware that notwithstanding any other provision of law, no person shall be subject to a penalty for failing to comply with a collection of information if it does not display a currently valid OMB control number.					
1. REPORT DATE 2008		2. REPORT TYPE		3. DATES COVERED 00-00-2008 to 00-00-2008	
4. TITLE AND SUBTITLE First-Principles Simulations of Violent Space-Weather Events				5a. CONTRACT NUMBER	
				5b. GRANT NUMBER	
				5c. PROGRAM ELEMENT NUMBER	
6. AUTHOR(S)				5d. PROJECT NUMBER	
				5e. TASK NUMBER	
				5f. WORK UNIT NUMBER	
7. PERFORMING ORGANIZATION NAME(S) AND ADDRESS(ES) Naval Research Laboratory, 4555 Overlook Avenue SW, Washington, DC, 20375				8. PERFORMING ORGANIZATION REPORT NUMBER	
9. SPONSORING/MONITORING AGENCY NAME(S) AND ADDRESS(ES)				10. SPONSOR/MONITOR'S ACRONYM(S)	
				11. SPONSOR/MONITOR'S REPORT NUMBER(S)	
12. DISTRIBUTION/AVAILABILITY STATEMENT Approved for public release; distribution unlimited					
13. SUPPLEMENTARY NOTES					
14. ABSTRACT					
15. SUBJECT TERMS					
16. SECURITY CLASSIFICATION OF:			17. LIMITATION OF ABSTRACT Same as Report (SAR)	18. NUMBER OF PAGES 9	19a. NAME OF RESPONSIBLE PERSON
a. REPORT unclassified	b. ABSTRACT unclassified	c. THIS PAGE unclassified			

within the Sun's forbiddingly harsh atmosphere. This forces us to infer many important clues using remotely sensed solar data from ground- and space-based telescopes and interplanetary data from satellites sampling ejecta that are already well on their way to the Earth. Nevertheless, as we describe below, progress toward the necessary physical understanding is being made, laying the foundation for future physics-based forecasting. Our first-principles computational model can simulate the approach to, onset, and aftermath of the violent magnetic explosions at the heart of the most extreme space weather.

A VIOLENT SPACE-WEATHER EVENT

A well-observed example of such a solar storm is shown in Figures 1 and 2. It occurred on 30 July 2005, during the most magnetically active epoch of the current sunspot cycle. Figure 1 shows the source region of the storm as seen in ultraviolet light by the Transition Region And Coronal Explorer (TRACE) satellite. Light and dark regions in the image correspond to hotter and cooler plasmas, respectively, residing in the corona, the tenuous outer layer of the Sun's atmosphere. Clearly visible over much of the field of view are arching threads of plasma, some very bright and others rather dim, which are understood to delineate magnetic loops from strong sunspot and weaker background fields at the solar surface. Less obvious but also visible are very dark threads, associated with cool plasma distributed along other, very low-lying magnetic field lines. These filamentary fragments can be seen in the first two panels of Fig. 1, below the long bright thread marked by the arrow in the second panel (top middle) and in the near left of the emitting region in the first panel (top left); the latter subsequently is replaced by the short canopy of bright loops in the foreground. A time-lapse movie of these images shows that the dark filament material is ejected upward and to the right, which is the solar north direction, during this sequence beginning at about 0620 UT. A small, bright kernel of hotter plasma, marked by the arrows (white) in four successive panels, is ejected along with and accompanies the filament. The overall rapid brightening of the plasma, observed in higher energy X-rays as well as the ultraviolet, is due to heating by the magnetic field. At the end of the ejective phase (bottom right), a very bright canopy of loops overlies the whole sinuous inverse-S shaped channel previously occupied by the dark filament. The impulsive phase of this eruptive flare has concluded, and thereafter the emission from the hot flare loops fades gradually as the plasma cools in place.

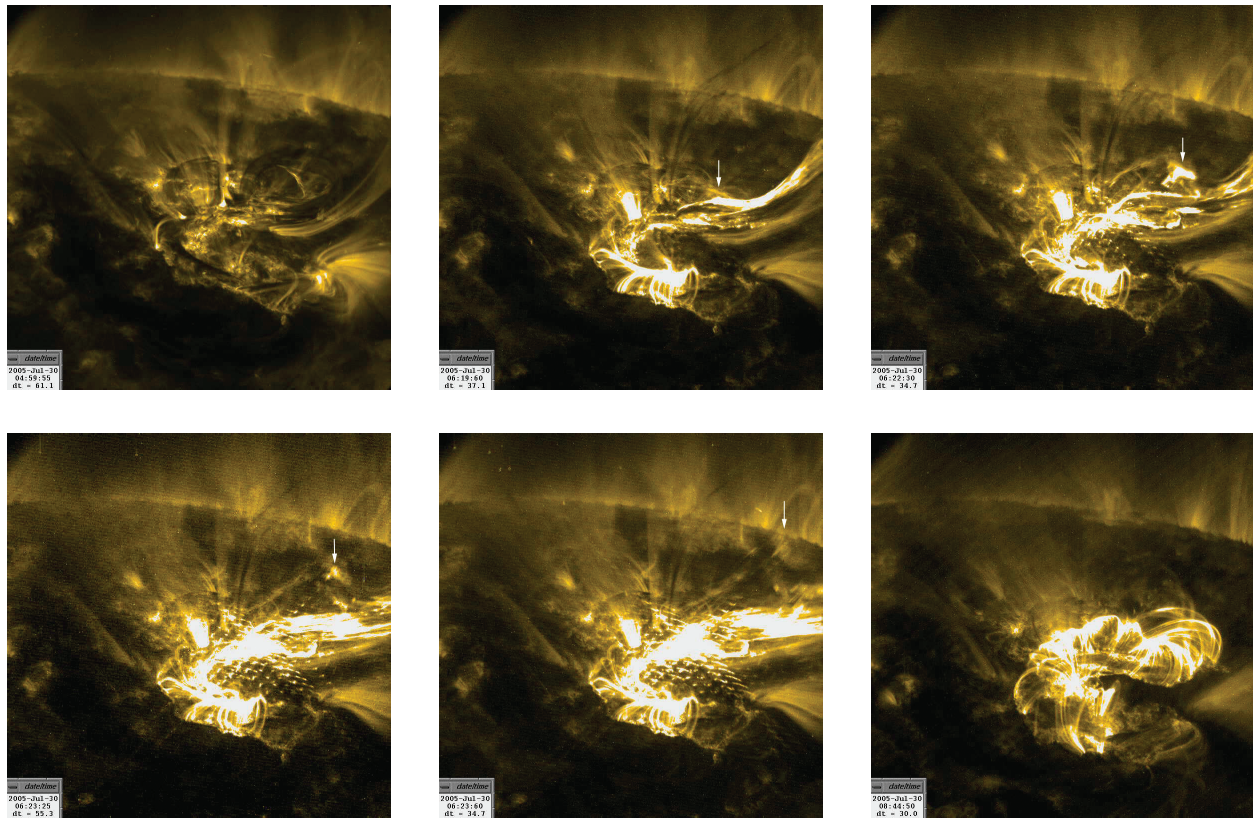
The initial development of the interplanetary consequences of this event are shown in Fig. 2, as observed

in scattered white light by the Large Angle Spectrometric CORonagraph (LASCO) instrument—whose design and development were led by NRL—on the SOLar and Heliospheric Observatory (SOHO) spacecraft. As is typical during that epoch, the background outer corona comprised several bright streamers of relatively dense plasma separated by expanses of tenuous plasma that scatters little light and so is quite dim. This sequence of panels shows two distinct explosions off of the limb of the Sun at about the 10 o'clock position. The first reaches its maximum brightness at about 0650 UT (top middle), a half hour after onset of the TRACE filament eruption, and its extent at this time suggests a speed of at least 500 km s^{-1} measured against the plane of the sky. Clearly, this coronal mass ejection (CME) expelled a large amount of plasma from the Sun into interplanetary space. About two hours later (top right), a very elongated, slightly twisted, bright thread is visible in the wake of the explosion. Thereafter, the corona relaxed (bottom left) back to essentially its configuration prior to the eruptive flare and CME (top left). A second CME, originating in the same source region, followed the first after an 11-hour delay and can be seen in the last two panels (bottom middle and right) of Fig. 2. Such multiple eruptions from a single source are certainly not unheard of, although a longer delay of up to a few days between successive occurrences is more common. Although these two CMEs departed the Sun too near the limb to have any large terrestrial impact, this is merely an accident of timing: three days later, their source region was much closer to disk center, and Earth likely would have been in the path of the storm as it has been on so many other occasions.

The eruptive flare and its associated coronal mass ejection described here are fairly typical solar events. Their signatures are common to essentially all large-scale disturbances of space weather, although the absolute and relative magnitudes of the flare and CME vary significantly across the spectrum of eruptions. The objective of our research is to understand these signatures, qualitatively and quantitatively, and to reproduce them as completely as we can in first-principles numerical simulations based on a compelling and robust physical model.

FIRST-PRINCIPLES SIMULATIONS

To advance understanding of the physics of eruptive flares and coronal mass ejections, we have developed and use two principal tools: the Adaptively Refined Magnetohydrodynamics Solver (ARMS), which performs detailed computer simulations of magnetized plasmas based on fluid-dynamical equations; and HelioSpace, which visualizes the numerical data from ARMS for interpretation and analysis. There are

**FIGURE 1**

Transition Region And Coronal Explorer (TRACE) images in 171 nm ultraviolet light of an eruptive flare that occurred on 30 July 2005. Solar north is to the right, and the limb is visible in the background. The quiescent pre-eruption state is shown at about 0500 UT (top left); the stable post-eruption state with glowing hot flare loops is shown at about 0845 (bottom right). In the intervening closely-spaced panels beginning at about 0620, a sinuous filament is ejected rapidly outward and in the northerly direction. A bright kernel of plasma in the ejecta, marked by the white arrows, cools and dims as it departs toward the upper right. The regular striations clearly visible in the last two of these panels are due to diffraction effects. A movie of the flare can be viewed at http://trace.lmsal.com/POD/movies/T171_20050730_03X.mov.

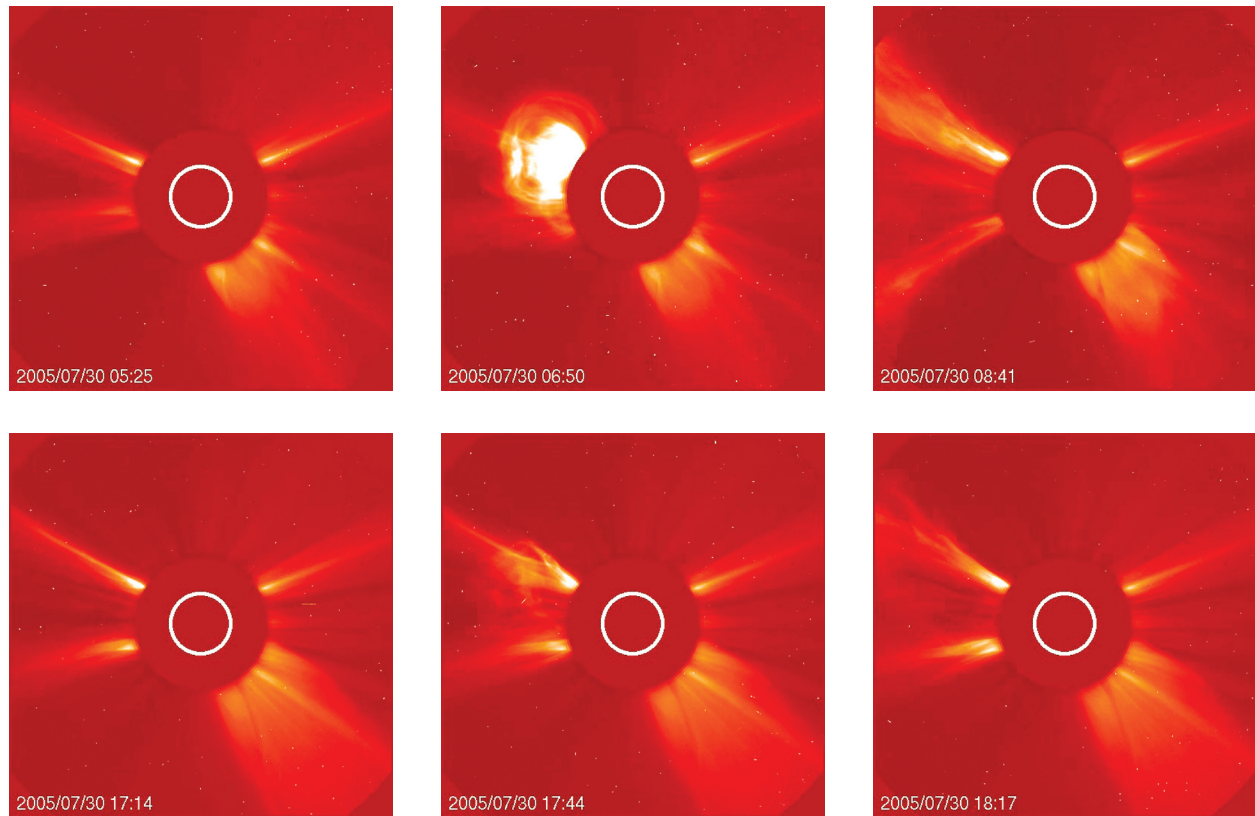


FIGURE 2

Large Angle Spectrometric CORonagraph (LASCO) images in scattered visible light of two coronal mass ejections (CMEs) that occurred on 30 July 2005. Solar north is at the top. The bright ring (white) at each image center represents the solar limb, while the larger dark circle is the occulting disk of the LASCO telescope. The quiescent pre-eruption states are shown at 0525 UT (top left) and 1714 UT (bottom left); the remaining two panels in each row show the ejected material moving outward from about the 10 o'clock position on the disk. This is the location of the TRACE filament eruption (Fig. 1), which closely precedes, and clearly is responsible for, the first CME shown here (top row). The second CME eleven hours later originated in the same source region, but TRACE unfortunately did not capture the associated flare. A movie of the CMEs is available at http://lasco-www.nrl.navy.mil/daily_mpg/2005_07/050730_c2.mpg.

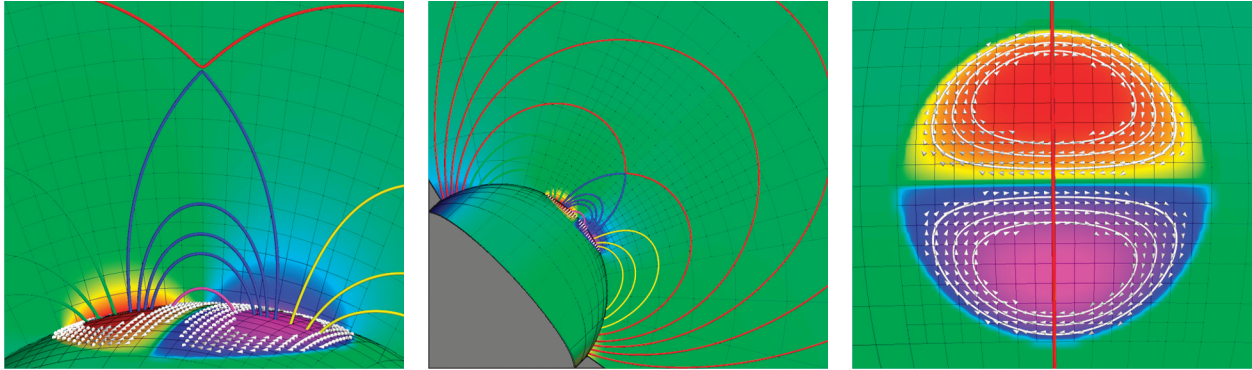
certain analogies between ARMS and sophisticated numerical models for global terrestrial weather: both solve for the large-scale, long-time behavior of their constituents using fluid equations that represent all three spatial dimensions and time, subject to the inertia of the medium and to pressure and gravitational forces. ARMS does not include the topographical and thermodynamic complexities that are so critically important to Earth's weather, but it does have to treat the critically important solar magnetic field and its associated forces on the plasma, which add their own numerical challenges. The resulting magnetohydrodynamics equations are solved using an extension of NRL's venerable Flux-Corrected Transport techniques for computational fluid dynamics. ARMS also employs adaptive mesh refinement, in which the numerical grid can be tailored to the problem being solved in order to use computational resources most efficiently, and it has been implemented on massively parallel computers, so as to harness the power of hundreds or even thousands of processors working together in synchrony to solve these complex problems. We must be able to visualize the resulting torrent of numbers effectively and in many different ways in order to interpret and understand them. HelioSpace accomplishes this with an intuitive user interface that offers several different rendering modules. It runs under all currently popular operating systems for desktop workstations and portable laptop computers.

A recent ARMS simulation of an eruptive flare and coronal mass ejection, visualized by HelioSpace, is initialized as shown in Fig. 3. The configuration is a large pair of semicircular sunspots, one on either side of the equator, embedded in the Sun's global background magnetic field, which is concentrated toward polar latitudes. The spherical solar surface, color-shaded according to the strength and sign (negative: red to yellow; positive: blue to magenta) of the radial component of the magnetic field, is seen at the bottom in the close-up view (left), from the side in the limb view (middle), and from above in the overhead view (right). A plane cutting radially through the central meridian is similarly color-shaded in the first two views. On both surfaces, we also draw lines (black) showing the boundaries of the $8 \times 8 \times 8$ blocks that make up the computational grid. These lines are most concentrated in the inner volume of the close-up view and become increasingly sparse farther away, since we have adapted the grid to resolve well only the anticipated region of principal activity. Also shown on the spherical surface are arrows and streamlines (white) of a flow that we impose there in our simulation; its purpose is discussed below. Finally, each thin cylindrical tube threading through space represents a selected individual magnetic field line. Its color is determined by the surface patches

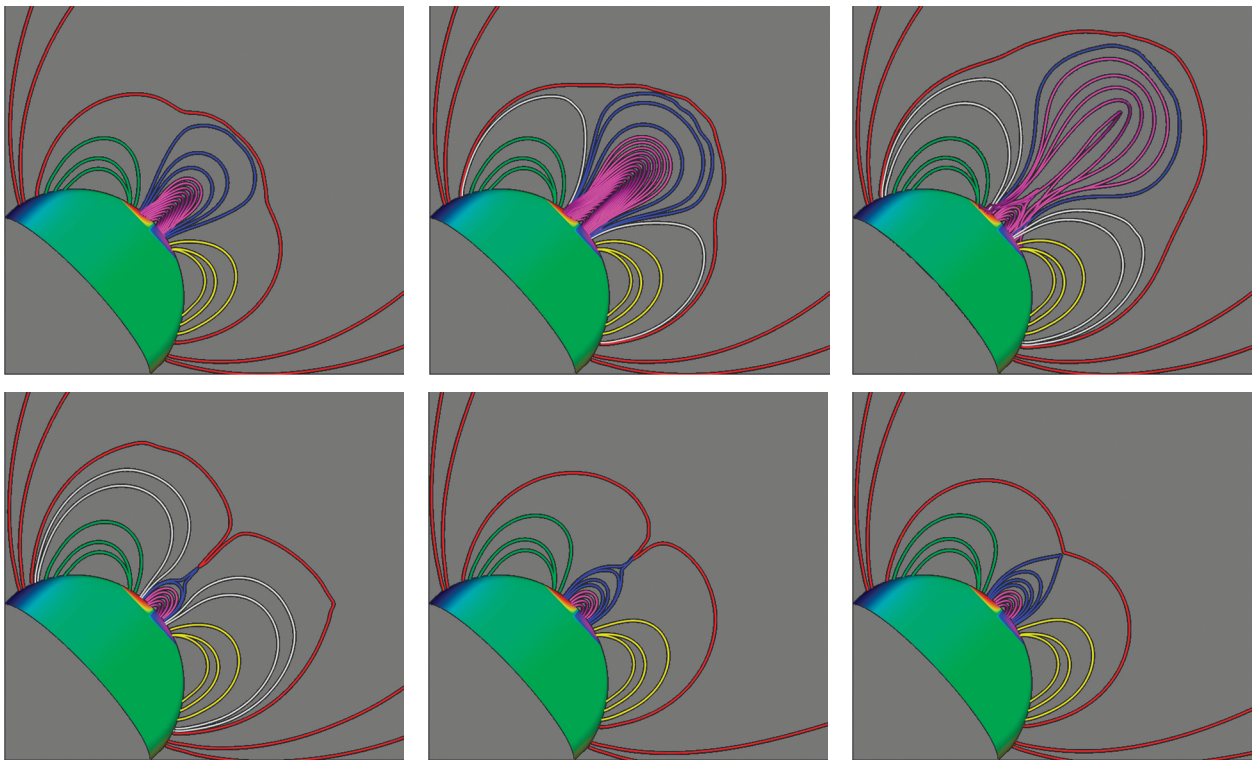
of positive and negative radial magnetic polarity at the two endpoints that are linked by that field line. We then can distinguish readily between lines that close locally across the equator and link the two sunspots (blue) from those that close remotely across the equator and link the two polar caps (red), as well as those that close within each hemisphere and link each polar cap to the nearer sunspot (north: green; south: yellow). We further distinguish the innermost equatorial field lines (magenta) whose endpoints reside within the zone of imposed surface motions from those farther out (blue) whose endpoints reside beyond that zone.

This initial field contains the minimum magnetic energy that is consistent with the prescribed distribution of sunspot and polar-cap magnetic flux at the surface. Field lines linking the two sunspots near the boundary between them—such as the one (magenta) shown in Fig. 3, and others like it at both higher and lower latitudes and at longitudes all along the extended boundary—cross over at a 90° angle and so are relatively short. In contrast, the source regions that spawn eruptive flares and coronal mass ejections invariably contain field lines that cross over their boundaries at a quite shallow angle and are very extended along those boundaries. The dark filaments pointed out in the TRACE image (Fig. 1) are comprised of such strongly sheared field lines. It is well known that sunspot rotation is an important contributing factor to the development of such lines of magnetic force, in at least some solar source regions. Thus, in our simulation model we impose clockwise rotational motions near the perimeters of the sunspots, as shown in Fig. 3. These motions gradually stretch the affected field lines (magenta) near the boundary between the sunspots, performing mechanical work that adds energy to the magnetic field. Indeed, it is this excess magnetic energy—above the minimum contained in the initial field configuration—that ultimately powers the eruption. The key issue is whether that excess energy can be converted to lift the plasma against gravity and accelerate it to high speed in the CME, and to heat the plasma on the bright loops left behind in the eruptive flare.

As the magnetic field adjacent to the boundary between the sunspots is stretched and its energy increases due to the rotational motions, the volume occupied by it expands, especially radially outward where the surrounding field is weakest. This is illustrated in the first panel (top left) of Fig. 4. The outward expansion of the increasingly sheared innermost field lines (magenta) stretches out the overlying unsheared field lines (blue) so that the downward tension force exerted by the latter remains in balance with the upward pressure force exerted by the former. In addition, the expansion compresses and reshapes the region between the field lines that link the two sunspots

**FIGURE 3**

Initial configuration for the Adaptively Refined Magnetohydrodynamics Solver (ARMS) numerical simulation, in close-up (left), limb (middle), and overhead (right) views. Grid lines (black), flow lines and directional arrows (white), and radial magnetic field strength and sign (red to blue shading) are rendered on the model solar surface and on the central-meridian plane. The cylindrical tubes are magnetic field lines colored according to whether they link the two sunspots (blue), the two polar caps (red), or a sunspot to the polar cap in its own hemisphere (north: green; south: yellow), or reside deep within the sunspot pair (magenta) and are subjected to the energizing surface flows.

**FIGURE 4**

Magnetic-breakout eruption from the ARMS numerical simulation, whose initial field configuration is shown in Fig. 3. The first three panels (top row) illustrate the accelerated eruption of the originally low-lying magnetic field lines (magenta) and plasma; the last three panels (bottom row) show the subsequent formation of the flare loops and the reestablishment of the original overlying equatorial (blue) and polar (red) field-line populations. Field lines with new connections (white) are created during the eruption and then destroyed during the flare. The time cadences are 20 minutes between the first four panels, then one hour to the fifth panel, and finally two hours to the sixth panel.

(blue) and those that link the two polar caps (red): the X-shaped intersection of the initial configuration (Fig. 3) evolves into a flattened plane interface that is very extended latitudinally in the strongly energized configuration (Fig. 4, top left). Note that the field lines in these two populations are antiparallel, since those linking the sunspots point northward, exiting the Sun from the southern sunspot and reentering the Sun in the northern sunspot; meanwhile, those linking the polar caps point southward, exiting from the north pole and reentering in the south pole. This antiparallel alignment permits pairs of these field lines to break and establish new connections with each other, exchanging endpoints in the process. These newly formed field lines (white) link each sunspot to the polar cap in its own hemisphere, as seen in the second and third panels (top middle and right).

The breaking and reconnecting of the overlying field is critically important to the eruption, because the tension force exerted by the original pairs of field lines upon the stressed field rising from below has been eliminated. The newly formed field lines do not overlie the rising energized field, and so can be pushed aside quite easily. Moreover, this process runs away catastrophically due to a positive feedback: reducing the tension force overlying the energized field allows it to rise faster and farther, which drives even faster reconnection of the residual field above it, which in turn reduces the tension force still more rapidly. As can be seen by comparing the heights of the energized field lines (magenta) across the top row of panels in Fig. 4, the result is a strongly accelerated outward expansion of the originally low-lying magnetic field and plasma. This is precisely the outcome predicted by our “magnetic breakout” model for eruptive flares and coronal mass ejections.¹

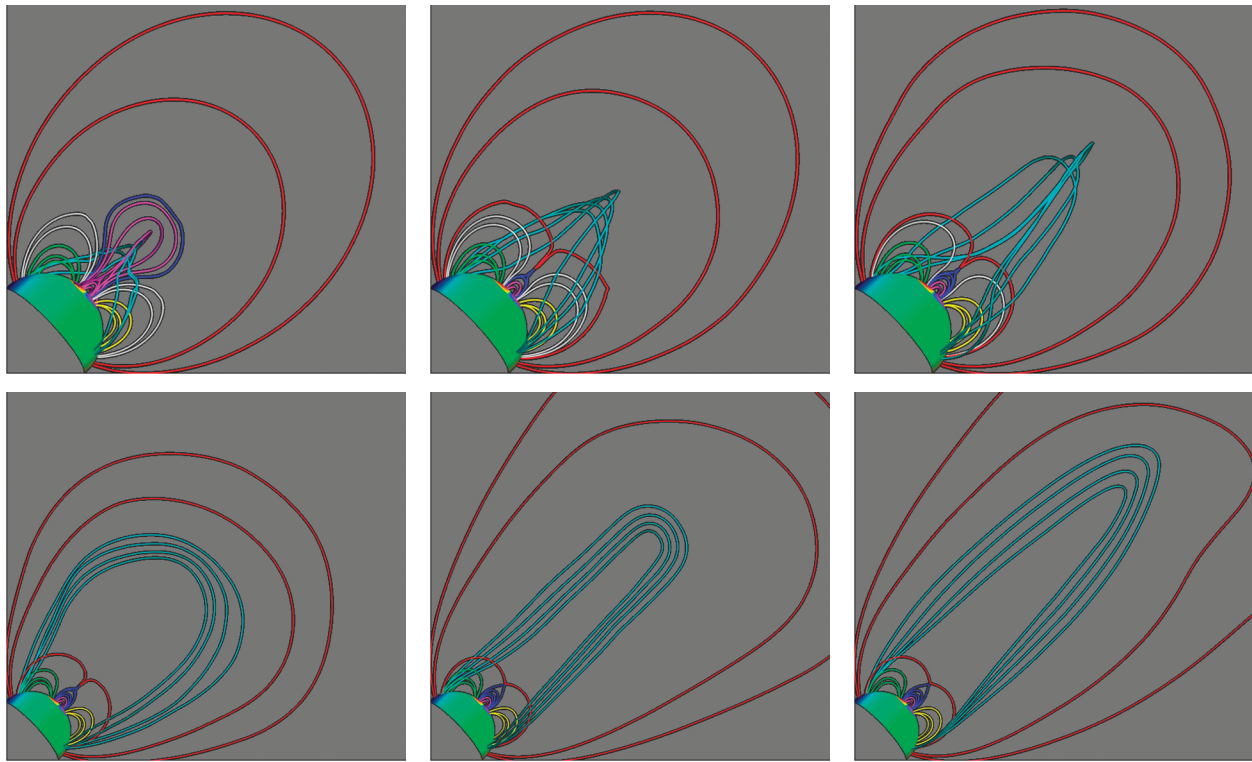
In the immediate aftermath of the eruption, field lines on both sides of the boundary between the sunspots are extremely elongated radially. Because these two populations of field lines also are antiparallel—pointing upward on the south side and downward on the north—they similarly suffer breaking and reconnecting. As they rebound back toward one another, following the impulsive outward escape of the energized field (magenta) from below, their original sunspot-linking (blue) and polar-cap-linking (red) connections get restored. This process is illustrated across the bottom row of panels in Fig. 4. The newly reformed, sunspot-linking field lines (blue) host plasma that has been heated during the breaking and reconnecting process, so that they constitute the hot loops which accompany eruptive flares (Fig. 1). The final, fully relaxed configuration at low heights in our simulation (Fig. 4, bottom right) rather closely resembles the minimum-energy configuration with which we

started (Fig. 3). This, too, is typical of solar eruptions: the considerable excess magnetic energy contained in the pre-event field is mostly absent from the post-event field, having been converted to energy of the plasma by the eruption.

The larger-scale, interplanetary consequences of the simulated eruption are shown in Fig. 5, which examines the magnetic field from more remote vantage points. In the first panel (top left), newly formed field lines (cyan) link the north and south polar regions, threading through the heart of the strongly energized field lines (magenta) that are in their rapid rise phase. Yet a third breaking and reconnecting process is responsible for their generation.² These new field lines comprise a giant, mildly twisted, transequatorial loop. As can be seen in the rest of the panels, this loop thereafter escapes the Sun into interplanetary space. Because the number of turns in the loop is fixed, as it lengthens, the twist per unit length drops and the loop becomes increasingly straight in appearance. Such mildly twisted CMEs are routinely measured in the solar wind by spacecraft and have been called “magnetic bottles,” to contrast them with the equally plentiful “flux rope” interplanetary CMEs that are much more strongly twisted and so resemble loosely wound springs. In the last panel of Fig. 5 (bottom right), the leading edge of the ejected magnetic bottle is slowing and losing some energy as it increasingly stretches the overlying polar-cap magnetic field lines (red) ahead of it. Nevertheless, the CME is still outbound at this time and more than eight solar radii from the Sun, a mere four hours after onset of the magnetic-breakout eruption.

CONCLUSIONS

The results of this first-principles numerical simulation are encouragingly consistent with the essential qualitative features of eruptive solar flares and coronal mass ejections. Also, although we stress that it is far too simple and abstracted to serve as a quantitative model for any real space weather event, it is nevertheless true that it yields approximately “a billion tons of matter moving at a million miles per hour.” These qualitative and quantitative successes give us confidence that our line of attack is a fruitful one and that our intuitive physical understanding of the genesis of the most violent space weather is sound. Many other, closely related simulations have been done, are under way, or are planned for the near future. Their aims are to advance us toward more realistic, complex, and challenging simulations of individual events, and to provide a comprehensive, quantitative grasp of how the characteristics of the source region determine the properties of the resultant disturbance. We also are examining our results to discern additional details of the observational

**FIGURE 5**

Magnetic-breakout eruption from the ARMS numerical simulation, viewed from more remote vantage points than in Fig. 4. The first panel (top left) shows the long transequatorial loop field lines (cyan) newly formed during the rapid rise phase of the eruption; these field lines and their entrained plasma subsequently escape the Sun as the coronal mass ejection. Note the scale change between the first and second rows of images. The last panel (bottom right) is at the same time as the last panel in Fig. 4, that is, four hours after eruption onset.

signatures predicted by the model, which have potential application to forecasting as well as a vital role in validating our approach. Given the required foundation of physical understanding, space-weather forecasting—like that of terrestrial weather before it—could be poised to make the transition from a basic research enterprise to a valued economic, national security, and military asset.

ACKNOWLEDGMENTS

The research underlying these results has received sustained support over a number of years from the Office of Naval Research through NRL's 6.1 Core program and from the National Aeronautics and Space Administration through its numerous programs in heliophysics. The DoD High Performance Computing Modernization Program similarly has provided extensive computer resources at several sites for our computations, and its Common High-Performance-Computing Software Support Initiative funded the development of our state-of-the-art numerical tools.

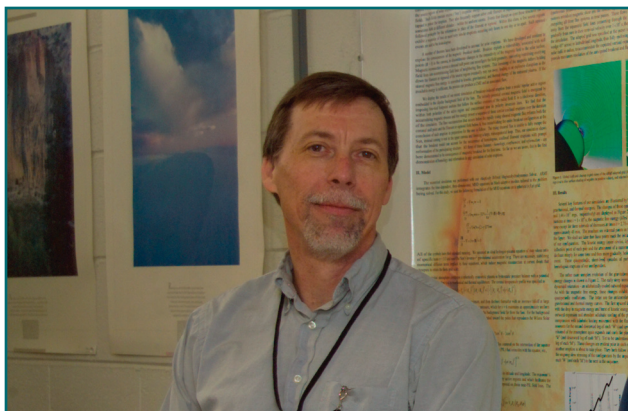
We are grateful to Peter J. MacNeice and Kevin M. Olson for their vital contributions to the ARMS simulation model, Timothy J. Hall for his expert work on the HelioSpace visualizer, Jean E. Osburn and Portia K. Shingler for their able administration of our computer allocations, and James A. Klimchuk and Benjamin J. Lynch for many stimulating discussions on the physics of CMEs. We also acknowledge use of images from TRACE, a NASA Small Explorer mission run by the Stanford-Lockheed Institute for Space Research, and the LASCO telescope aboard SOHO, which is a joint mission of the European Space Agency and NASA.

[Sponsored by NASA and ONR]

References

- ¹S.K. Antiochos, "The Magnetic Topology of Solar Eruptions," *Astrophysical Journal* **502**, L181 (1998); S.K. Antiochos, C.R. DeVore, and J.A. Klimchuk, "A Model for Solar Coronal Mass Ejections," *Astrophysical Journal* **510**, 485 (1999).
- ²C.R. DeVore and S.K. Antiochos, "Homologous Confined Filament Eruptions via Magnetic Breakout," *Astrophysical Journal* **680**, 740 (2008). ★

THE AUTHORS



C. RICHARD DEVORE has been a staff member in the Laboratory for Computational Physics and Fluid Dynamics at NRL since 1983. He received his Ph.D. in astrophysical sciences from Princeton University in 1986. His research interests include numerical magnetohydrodynamics and plasma physics, parallel computing, and adaptive mesh refinement, particularly as applied to space weather. Dr. DeVore is a Fellow of the American Physical Society.



SPIRO K. ANTIOCHOS became a staff member, and later head, of the Solar Theory Section in the Space Science Division's Solar-Terrestrial Relationships Branch at NRL in 1985. He received his Ph.D. from Stanford University in 1976, and was a research associate there prior to his arrival at NRL. Dr. Antiochos' research spans much of solar physics, with an emphasis on developing theories and simulations to account for a wide range of observed phenomena. For his important and fundamental contributions to the field, he received its highest honor, the George Ellery Hale Prize of the American Astronomical Society, in 2005. Dr. Antiochos is an E.O. Hulburt Award winner at NRL, a Fellow of the American Geophysical Union, and an honorary member of the Royal Astronomical Society. In early 2008, he assumed the post of Senior Scientist for Space Weather at NASA Goddard Space Flight Center in Greenbelt, MD.